ROTOR BLADE TIP SWEEP EFFECT ON LEAD-LAG DAMPING IN HOVER AND FORWARD FLIGHT

Lokeswara Rao. V[1]
[1]Ph.D. Candidate, IIT-Kanpur
Senior Manager (Design),
Rotary Wing Research and Design Center,
Hindustan Aeronautics Limited,
Bangalore-560037, India
lokeshv@iitk.ac.in

C. Venkatesan*[,2]
*Former HAL Chair Professor, IIT-Kanpur
[2]Visiting Professor
Department of Mechanical Engineering
Indian Institute of Technology,
Jodhpur-342037, India
cven@iitj.ac.in

Abstract

Rotor blade geometry (tip sweep, planform taper and anhedral) significantly influences the aerodynamic efficiency, vibratory loads and aeroacoustic behavior of the helicopter rotor. In this paper, the focus is on analyzing the effect of blade tip sweep on the structural dynamic, aeroelastic loads and blade lead-lag damping in hover and forward flight for an isolated rotor. For carrying out this analysis, a comprehensive analytical model is developed. In the structural model blade undergoes coupled flap, lag, torsion and axial deformations. Tip sweep, pretwist, precone, predroop, torque offset and root offset are included in the model. Aerodynamic model includes 3-state Peters-He dynamic wake theory for inflow and the modified ONERA dynamic stall theory for airloads calculations. The comprehensive model is first validated by comparing the predicted results with experimental data. The predicted results of blade root loads and lag damping for a straight blade in hover, over the collective angle settings of -2 to 6 degrees, are in a very good agreement with the measured whirl tower test data. In hover and forward speeds, the lag damping values of swept tip blade are less compared to the straight blade for various collective angle settings. For a straight blade, lag damping values show slight increase and decrease with the increase in advance ratio, whereas for the swept tip blade, lag damping shows a marginal increase at lower advance ratio up to 0.1 and then a decrease in the range of advance ratios 0.1 to 0.2 and thereafter it shows an increasing trend. This kind of variation in damping trends for straight and swept blades with forward speed qualitatively agrees with experimental observations available in the literature.

NOMENCLATURE

Symbols

a	torque offset
e_1, e_2	root offset
β_d	blade predroop angle
β_p	blade precone angle
β_s	blade presweep angle
Λ_a	tip anhedral angle
Λ_s	tip sweep angle
$[\bar{M}]$	mass matrix in modal space
$[\bar{C}]$	damping matrix in modal space
$[\bar{K}]$	stiffness matrix in modal space
$\{\eta\}$	vector of modal degree of freedom
$\{\bar{F}\}$	generalised load vector
$\{F_{AD}\}$	aerodynamic force vector
$\{q\}$	finite element nodal displacement
$[\Lambda]$	sweep,anhedral transformation matrix
X_k	coordinate along kth blade axis
Ω	rotational frequency of the rotor

Subscripts

$(\,)_{1k}$	quantities in rotating 1k system
$(\,)_{2k}$	quantities in rotating 2k system
$(\,)_{3k}$	quantities in rotating 3k system
$(\,)_{4k}$	quantities in rotating 4k system
$(\,)_e$	quantities in rotating e system
$(\dot{\cdot})$	derivative w.r.t. time

Presented at 47th European Rotorcraft Forum, United Kingdom, 7-9th September, 2021

1. INTRODUCTION

Helicopter rotor blades operate in a highly complex unsteady aerodynamic environment. Tip geometry of the rotor blade plays a significant role in influencing the rotor performance. Tip sweep, tip anhedral and the planform taper of the tip are used as important design parameters in improving the rotor performance. Tip shape influences the blade-vortex interaction and significantly affects the aerodynamic and aeroacoustic behavior of the rotor[1-3]. Experimental studies have been carried out to evaluate the influence of tip geometry on the rotor performance and rotor loads[4,5]. These advanced geometry rotor blades are receiving increasing attention by the designers as a viable means to alleviate drag rise, stall effects, and acoustic noise. In addition, it may be an attractive option for reducing vibratory hub loads and improving aeromechanical stability.

Several computational studies have been carried on the aeroelastic and dynamic characteristics of rotor blades with advanced tip geometry. Tarzanin and Vlamick[6] analysed the articulated rotor vibration and stability characteristics with blade tip sweep. Celi and Friedmann[7] formulated a refined structural model for swept tip hingeless rotor blades. The blades were modeled by defining the elastic axis as the line joining the shear centers of the cross sections of the blade. Linear transformations were used at the junction of straight and swept portions. Panda[8] formulated the transformation relation between straight and swept tip junction, which is essentially nonlinear.

Kim and Chopra[9] presented the aeroelastic analysis of hingeless rotor blades equipped with both tip sweep and anhedral by adding the nonlinear transformation to combine the tip sweep with the straight blade. In Ref. [10], the authors studied the effect of tip sweep on the aeroelastic stability in hover and forward flight by combining the nonlinear moderate deflection beam theory with uniform inflow model. Bir and Chopra[11] formulated an aeromechanical stability model for a rotorcraft with advanced geometry blades. Their formulation included a general tip planform, arbitrary sweep, and anhedral.

Kumar and Venkatesan[12] formulated a computational aeroelastic model by integrating the structural model, dynamic wake model, and the dynamic stall models. They presented that the tip dihedral/anhedral combined with the tip sweep is influencing both the hub loads and the flight dynamics of the helicopter. Epps and Chandra[13] performed experimental studies to identify the effect of tip sweep on the natural frequencies of rotating beams made of either aluminum or graphite epoxy composite material. Tip sweep angles of 15 deg., 30 deg., and 45 deg. are considered in the experimental study. Theoretically estimated natural frequencies were compared with the experimental data. Ormiston and Hopkins[14] developed and validated a nonlinear finite element model for swept tip rotor blades considering large defections. It is based on the theory by Hodges and Dowell[15]. Amoozgar, et al.[16] presented the dynamics of a composite rotating blade with the curved tips (out-of-plane, in-plane). The composite blade is modeled by using the exact beam formulation. Their studies show that the curved tip of the blade affects the blade frequencies due to extra couplings.

BERP (British Experimental Rotor Programme) rotor demonstrated the capability to provide high speed performance[17] and it led to the development of double sweep rotor blade concepts (ERATO, BLUE EDGE^{TM}),[18,19] which seem to be more attractive and promising. Truong[20] investigated the influence of double sweep on the modal characteristics (modal frequencies and modal contributions) of the ERATO blade. Kumar and Rao[21] pointed out that double-swept geometry caused large lag shear forces and torsional moments at the blade root, as well as at the double-swept junction. Filippi et al.[22] used the multidimensional finite element model to study the modal characteristics of a double-swept blade.

In Ref. [23], the authors investigated the influence of double-swept parameters including the inner swept-forward angle, outer swept-back angle, outer droop angle, and junction position on the aeromechanical stability in ground contact condition and also in forward flight condition. All these studies were focused on the aeroelastic stability and aeromechanical stability of the rotor blade coupled with fuselage for single-swept / double swept tips. There is limited literature on the effect of sweep on lag damping of the blade.

Maier et al.[24], have performed an experiment on straight and 30 deg. swept-back tip rotor blade models to evaluate the influence of tip sweep on lead-lag damping in hover and forward speed. The experimental results were also compared with theoretical results generated using a comprehensive analysis tool. The key observations of this study are: for straight blade, the predicted lag damping over the entire collective range shows a very good agreement with the measurement. However for the swept blade in forward flight, the predicted lag damping values are significantly higher compared to the measured values at higher collective angle settings (Figure 24 of Ref. [24]). The measured damping values for swept tip blades show a marginal variation with forward speeds

Presented at 47th European Rotorcraft Forum, United Kingdom, 7-9th September, 2021

whereas the theoretically predicted values show a significant increase in damping particularly at higher collective angles.

The present study aims to understand the effect of tip sweep on lag damping, and blade root loads, of a realistic helicopter rotor blade. This study is an extension of the comprehensive aeroelastic and flight dynamic analysis of rotorcraft (CAFDAR) developed in Refs. [12 and 21]. The objectives of the present study are:

(i) Formulation of an aeroelastic model applicable for a realistic hingeless rotor blade with tip sweep.

(ii) Validation of the structural dynamic part of the aeroelastic formulation by comparing the theoretically predicted natural frequencies with the experimentally measured natural frequencies of a rotating composite beam with tip sweep.

(iii) Validation of the aeroelastic model by comparing the theoretically predicted values with whirl tower measurements in thrust, power, blade root loads and lead-lag damping for different collective pitch angles of a straight blade.

(iv) Evaluate the effect of tip sweep on lag damping in hover and forward speed for various collective pitch angles.

2. COMPREHENSIVE AEROELASTIC MODEL

The complete aeroelastic model requires the formulation of equation of motion, representing the structural dynamic model of the rotor blade, aerodynamic model for the evaluation of the sectional loads on the blade and rotor inflow model. The structural and the aerodynamics models used in the helicopter aeroelastic analysis have been described in detail in Ref. [25].

2.1. Blade structural model

The elastic rotor blades are idealized as long, slender beams undergoing moderate deformations in axial, bending and torsional modes. The coupling effects between axial, bending and torsional deformations, transverse shear and out of plane warping characteristics of the blades are included in this formulation. The rotor blade with most general geometry is shown in Fig. 1.

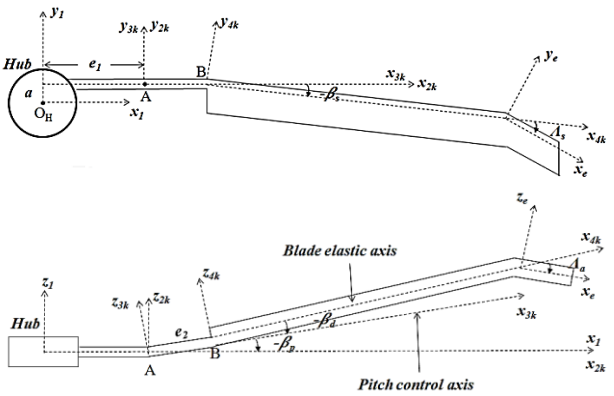

Figure 1: Rotor blade co-ordinate systems

Blade sweep, precone, predroop, pretwist, root offset and torque offset are included in the model. The beam consists of a straight portion and a tip with sweep and anhedral angles relative to the straight portion.

The nonlinear equations of motion and the corresponding finite element matrices were derived for each beam element using Hamilton's principle. The blade was modeled by a series of straight-beam finite elements along the elastic axis of the blade. Each finite element in the tip can be given a sweep angle and/or anhedral angle independent of the other. Each beam element consists of two end nodes and one internal node at its mid-point, resulting in 14 degrees of freedom representing four lag, four flap, three torsional and three axial deformations. Cubic Hermite interpolation polynomials are used for the bending displacement, while quadratic Lagrangian interpolation polynomials are used for torsional rotation and axial deflections. The linear, undamped model is solved in the finite element domain to obtain the natural frequencies and the corresponding mode shapes of the rotating blade. The governing equation for the i^{th} finite blade element is

$$[\mathrm{M_i}]\{\ddot{\mathrm{q}}_\mathrm{i}\}+[\mathrm{K_i}]\{\mathrm{q_i}\}=0 \quad (1)$$

Where $[\mathrm{M_i}]$, $[\mathrm{K_i}]$ represents mass and stiffness matrix of the i^{th} element.

For rotor blades with a sweep and/or anhedral, the governing equation for the corresponding blade element is given by

$$[\Lambda]^T[\mathrm{M}_i][\Lambda]\{\ddot{q}_i\}+[\Lambda]^T[K_i][\Lambda]\{q_i\}=0 \quad (2)$$

Where $[\Lambda]$ is the local-to-global transformation matrix for blade elements with sweep and anhedral.

Presented at 47th European Rotorcraft Forum, United Kingdom, 7-9th September, 2021

2.2. Aerodynamic model

The aerodynamic model involves the evaluation of inflow at various locations on the rotor disc and the evaluation of sectional aerodynamic loads on the rotor blade. The comprehensive aeroelastic and flight dynamics analysis of rotorcraft (CAFDAR) model has been developed and it has multiple options for inflow and load calculations. In this study, the rotor inflow is modeled using Peters-He dynamic wake model[26]; and the sectional aerodynamic loads (lift, drag and pitching moment) are evaluated using the modified ONERA dynamic stall equations[27]. Both these models, by virtue of being formulated as a set of differential equations, are very suitable for aeroelastic calculations.

The aerodynamic calculations are performed in the following manner: (1) The oncoming flow velocity at a section and the rotor inflow are first projected along the local coordinate system (eK) of that section. (2) The sectional loads are then calculated along this local coordinate system. (3) The loads are then transferred to 4K system which coincides with the local coordinate system for the straight portion of the blade. The transformation between the local (eK) and the 4K systems takes into consideration any sweep or anhedral angle at the section.

2.3. Numerical solution

The global aeroelastic equation for the whole blade is obtained by assembling the elemental matrices from the kinetic and strain energy contributions,

$$[\mathrm{M}]\{\ddot{q}\}+[\mathrm{C}]\{\dot{q}\}+[K]\{q\}=\{\mathrm{F_{AD}}\} \quad (3)$$

Where $\{\mathrm{F_{AD}}\}$ is the aerodynamic force contribution.

To reduce the number of degrees of freedom of the problem, modal co-ordinate transformation is performed on the aeroelastic equation. Eight modes comprising two lag, four flap, one torsion and one axial mode were used in the modal transformation. The equation of motion in modal space for aeroelastic calculations is

$$[\overline{\mathrm{M}}]\{\ddot{\eta}\}+[\overline{\mathrm{C}}]\{\dot{\eta}\}+[\overline{\mathrm{K}}]\{\eta\}=\{\overline{\mathrm{F}}\} \quad (4)$$

Where $\{\overline{\mathrm{F}}\}$ represents the generalized aerodynamic load vector.

The solution of the non-linear aeroelastic equation of the main rotor involves successively calculating the inflow, rotor loads and the resulting response for a small time step. The time is then incremented and the calculation process is repeated until the converged solution is obtained.

The present study is concerned with whirl tower analysis (isolated rotor). The flowchart in Figure 2 summarizes the procedure for whirl tower analysis. The loads, inflow and response equations are all in the form of differential equations and solved iteratively till a converged solution is obtained over several revolutions for a given set of rotor control inputs (collective and cyclic).

The blade equations and the aerodynamic equations are evaluated at alternate time steps for a whole revolution. The sectional aerodynamic loads are calculated at 15 prescribed equidistant stations on the rotor blades. The root loads are obtained by integration of the sectional loads over the length of the blade using Simpson's rule. The blade and aerodynamic differential equations were solved using the Runge-Kutta method. The analysis was implemented as a C++ program using the open-source GSL[28] as the math library. The simulation parameters and realistic rotor data for the whirl tower analysis is given in Table 1.

2.4. Damping estimation

Modal damping could be estimated using either logarithmic decrement technique, moving block technique or Prony curve fit method[29]. Applications have shown[30-32] that Time Domain (TD) analysis is appropriate in estimating the equivalent linear damping for linear or nonlinear vibratory systems. TD analysis correlates with the experimental data better than from Eigen analysis. TD analysis is a method of numerical solution that can simulate the experimental test procedures. In the present study, TD analysis methodology is considered for estimation of blade lead-lag damping. For experiment or TD analysis, estimation of damping is usually performed from transient responses time histories.

To estimate the blade lead-lag damping, in the aeroelastic model a cyclic excitation to each blade is given over steady collective input at a lag regressive frequency ($|\Omega-\omega_\zeta|$) in non-rotating frame. The lag regressive frequency in non-rotating frame will excite the blade lead-lag natural frequency (ω_ζ) in rotating frame. Cyclic excitation amplitude of 2 deg for 3 seconds is given and then stopped abruptly. Aeroelastic equation is solved iteratively till a converged solution is obtained over several revolutions for a given cyclic excitation over the steady collective input. From the converged solution, transient responses of all the blades are obtained.

Presented at 47th European Rotorcraft Forum, United Kingdom, 7-9th September, 2021

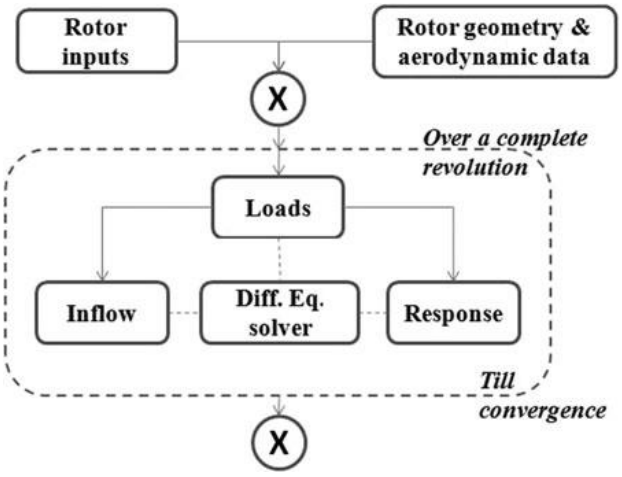

Figure 2: Flow chart for whirl tower analyses

Table 1: Rotor data

Parameters		**value**
Number of blades	N_b	4
Rotational speed	Ω (rad/sec)	38.43
Blade mass distribution	m_o (kg/m)	8.45
Non-dimensional blade chord	c/R	0.0621
Pre-Twist	(deg)	-10
Pre-flap	(deg)	2.5
Air density	ρ (kg/m^3)	1.224
Solidity ratio	σ	0.0737
Lock number	γ	9.72
Lift curve slope	$c_{l\alpha}$	5.73
Profile drag coefficient	c_{d0}	0.01
Torque offset	a	0.0014

A Multi Blade Coordinate (MBC) transformation is applied over the converged transient flap, lag and torsion responses of all the blades to obtain the responses of rotor modes (collective, cyclic and reactionless modes) in non-rotating frame. MBC can be performed as follows. For a rotor with N even number of blades and q_b be a particular rotating degree of freedom for the bth blade, the MBC is a linear transformation that relates a rotating degrees of freedom to the non rotating degrees of freedom as

(5) Collective mode: $$q_0 = \frac{1}{N}\sum_{b=1}^{N} q_b$$

(6) Cyclic mode: $$q_{nc} = \frac{2}{N}\sum_{b=1}^{N} q_b \cos n\psi_b$$

(7) Cyclic mode: $$q_{ns} = \frac{2}{N}\sum_{b=1}^{N} q_b \sin n\psi_b$$

(8) Reactionless mode: $$q_{N/2} = \frac{1}{N}\sum_{b=1}^{N} q_b (-1)^b$$

These non-rotating degrees of freedom represent the rotor degrees of freedom and they express the cumulative behavior of all rotor blades in the fixed frame. The $q_{N/2}$ mode exists only if number of blades is even. Blade damping is evaluated from the time responses of rotor modes using logarithmic decay technique. The logarithmic decrement represents the rate at which the amplitude of a free damped vibration decreases. It is defined as the natural logarithm of the ratio of any two successive amplitudes. The damping ratio (ξ) and logarithmic decrement (δ) are related as

(9) $$\delta = \frac{1}{m}\ln\left(\frac{x_1}{x_{m+1}}\right) = \frac{2\pi\xi}{\sqrt{1-\xi^2}}$$

X_1 and X_{m+1} are the amplitudes corresponds to times t_1 and $t_{m+1} = t_1 + mt_d$; m is the number of cycles and t_d is the decay time period.

3. WHIRL TOWER TEST SETUP

Rotor whirl tower tests are vital in the design and development of helicopter rotor system. These tests are used to evaluate structural and aeromechanical performance of rotor in hovering condition[33]. Precious information regarding dynamic balance, noise, aeroelastic stability, vibration and rotor performance as well as structural integrity of rotors at hover condition can be assessed in whirl tower tests.

Figure 3 shows the whirl tower test setup used for measuring realistic helicopter rotor performance characteristics (thrust, power, loads). The rotor blades are with straight tip geometry. In the current study, these test results were used for validation with CAFDAR analytical results. The data acquisition system allows for the real time measurement and record of critical parameters such as rotor torque, rotor rotational speed, thrust, blade flap, lag and torsional moments. Rotor blade unbalances and rig vibrations are also measured during the test. The rotor blade angle control system can be controlled steady-state or periodically in mono or multi-cyclic configurations by potentiometer inputs. The collective pitch control is totally separated from the cyclic input system. The collective pitch control is performed by moving the swashplate vertically with 3 booster rods which are equipped with linear actuators. For cyclic control

Presented at 47th European Rotorcraft Forum, United Kingdom, 7-9th September, 2021

and excitation, swashplate tilting is accomplished by a hybrid (electro-hydraulic) actuator. The hybrid actuator consists of a slow electrical linear motor with a self-locking ball screw drive flanged together with a dynamic electro-hydraulic actuator for small cyclic inputs. With the electrical linear actuator steady state cyclic inputs upto 3 deg. are applied at different collective angles. Blades are then in a forced flap excitation and are oscillating in resonance with the airloads in the first rotor harmonics. With periodical ($|\Omega-\omega_\zeta|$) input from the electro-hydraulic actuator, the first coupled regressing inplane mode of a blade is excited while rotor collective pitch is used to achieve desired thrust level. Inplane damping is derived from the decay curve of the inplane bending moment after stopping the excitation and calculating the damping ratio by applying the logarithmic decrement technique to the bending moment time trace.

Figure 3: Isolated rotor whirl tower test setup

4. RESULTS AND DISCUSSION

The results of this study are presented in three sections. In the first section, the results pertaining to the natural frequencies of a rotating composite beam are compared with the experimental data (from Ref. [13]). In the second section, a comparison of blade loads and lead-lag damping with measured data from whirl tower test of realistic straight helicopter rotor blade is presented. The third section presents the effect of tip sweep on the blade dynamic characteristics, loads and lead-lag damping.

4.1. Validation of structural dynamic analysis of swept-tip composite beam

Figure 4 and Table-2 show the geometric details of experimental graphite-epoxy composite beams with different tip sweep angles and ply orientation angles. The length of the swept portion is fixed at 15% of the total length (40 inch). The cross-sectional properties (mass, inertial and stiffness's) of aluminum and composite beams with different tip sweep and ply angles are evaluated using cross-sectional properties estimation tool (COPE)[34]. The evaluated sectional properties are given in Table 3. Natural frequencies of the beam for various sweep configurations are estimated using the structural dynamic model. The natural frequencies and mode shapes are evaluated for non-rotating and rotating (with 500 RPM and 750 RPM) configurations.

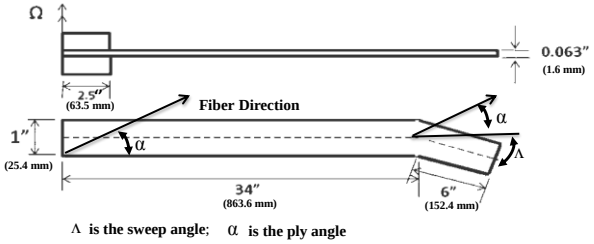

Figure 4: Geometric details of vacuum chamber experiment beam, Ref. [13]

The fundamental frequencies of the structural dynamic model are compared with the experimental data and they are shown in Figures 5 to 16. Figures 5 to 7 show the results pertaining to aluminium beam. The natural frequencies of the composite beams are shown respectively for different ply orientations in Figures 8 to 10 (for 0 deg. ply), Figures 11 to 13 (for 15 deg. ply) and in Figures 14 to 16 (for 30 deg. ply). It is observed from the figures that the estimated frequencies from the analytical model are in good correlation with the experiment values for various sweep angles and RPM configurations.

4.2. Validation of aeroelastic formulation (CAFDAR) with whirl tower test data

Isolated rotor whirl tower tests were conducted on a realistic hingeless straight rotor blade at HAL ground test facility to evaluate rotor performance. For validation of our aeroelastic model, the results of the theoretical formulation are compared with the whirl tower test data. To simulate a whirl tower test, aeroelastic analysis was carried out on a realistic isolated straight hingeless blade rotor for different collective angles (-2 deg to 10 deg). Rotor thrust, power and blade root loads are estimated from the

Presented at 47th European Rotorcraft Forum, United Kingdom, 7-9th September, 2021

converged solution. Figures 17 to 23 show the comparison of estimated rotor thrust, power and blade root loads (flap, lag and torsional moments) with the whirl tower test data.

It is seen from Figures. 17 and 18 that the thrust and power values from the analysis are matching with the test data fairly well. Figures 19 to 22 show the variation of root moments (#465 mm, # 850 mm) in flap, and lag for various collective pitch angles. Figure 23 shows the torsional moment variation with collective angle. Flap bending moment, lag bending moment and torsion moment correlate well with the measured data.

Lead lag damping characteristics of straight blade in hover condition are measured in whirl tower for collective angles of -2 deg. to 6 deg. In whirl tower a cyclic input is provided by an electro hydraulic actuator to excite the blade. A cyclic input of 2 degree amplitude is given at blade lag regressive frequency (2.1 Hz) and the lag damping is estimated from the time response of root lag moment using MBC transformation and logarithmic decay technique. Figures 24 and 25 respectively show sample cyclic input and blade response data of whirl tower and aeroelastic analysis (CAFDAR). The predicted and measured blade lag damping values are shown in Figure 26. It is observed that the predicted lag damping values show a good correlation with the measured values particularly at lower collective pitch angles. At higher collective angles the theoretically predicted damping values are slightly higher than the measured values.

4.3. Effect of tip sweep on blade dynamic characteristics, loads and lead-lag damping

In the present study, aeroelastic analysis is performed for a realistic hingeless blade with swept tip of 15 deg. and 30 deg. The length of the swept portion is fixed at 10% of the total blade length. The cross-sectional properties (mass, inertial and stiffness) are considered same as straight blade properties.

4.3.1. Effect of tip sweep on blade structural dynamic characteristics

Table 4 presents the influence of tip sweep on the blade natural frequencies. The first five modes show a decrease in natural frequencies with increase in tip sweep angle; whereas the sixth and seventh natural frequencies show a reduction in values. Tip sweep causes a shift in the centre of gravity (from the original straight elastic axis) of the swept part of the blade which in turn influences the blade torsional behaviour. The change in the natural frequencies is dependent on the magnitude of the swept angle and sweep lengths. Figures 27 and 28 respectively show the mode shapes of straight blade and 30 degree swept tip blade. It is clearly seen from the mode shapes (Figure 28) that blade tip sweep introduces bending-torsion couplings in the rotor blade.

4.3.2. Effect of tip sweep on blade blade performance and root loads

Figures 29 to 35 show the comparison of estimated rotor thrust, power and blade root loads (flap, lag and torsional moments) with blade sweep angles of 0(straight blade), 15 and 30 degree. From Figures 29 and 30, it can be seen that with increase in the sweep angles, there is a slight decrease in rotor thrust and power values. The magnitude of flap root moments decreases with increase in sweep angles, especially for positive collective angles (Figures 31 and 32). The root lag moments of swept tip blades show a downward shift compared to the straight tip blade for all collective angles (Figures. 33 and 34). A key observation, from Figs. 33 and 34, is that with increase in swept angle the zero cross-over point is shifting towards higher collective value. The magnitude of the root torsional moment shows an increase with collective angle both for low and high values. However for 4 deg. Collective, the torsional moment is not affected by tip sweep (Figure 35). The reason for these observed effects is due to the offset of the sectional aerodynamic centre and centre of gravity from the straight portion of the elastic axis of the blade. The aerodynamic lift and inertial forces acting on the swept blade introduces both pitch down and pitch-up moments about the straight elastic axis. Apart from this, the swept portion aerodynamic drag forces are inclined to the straight portion of the blade which reduces the aerodynamic drag component. Because of centre of gravity offset, centrifugal force has components contributing to the root lag and torsional moments.

4.3.3. Effect of tip sweep on blade lead-lag damping

Figure 36 shows the comparison lag damping variation with collective pitch for straight and swept tip blade. It is observed that lag damping amplitude decreases with tip sweep compared to the straight blade for the entire range of collective settings. Figures 37 to 39 show the variation of lag damping with forward speed for various collective pitch angles for straight and swept tip (15 deg. and 30 deg.) blades respectively. It is noticed in these figures that the damping values are increasing with

Presented at 47th European Rotorcraft Forum, United Kingdom, 7-9th September, 2021

increase in blade collective pitch for both straight and swept tip blades. Comparing the Figures 37 to 39, it can be seen that for a given collective pitch angle, the swept tip blade has less value of damping compared to the straight blade. With increase in advance ratio, for straight blade (Figure 37) the damping slightly increases and then decreases; whereas for swept tip blades (Figures 38 and 39), the damping increases initially and then decreases and again shows an increase. It is also noticed in Figures 38 and 39, the tip sweep marginally affects the lag damping of the rotor blade with respect to forward speed. A qualitative comparison of this result with the experimental data presented in Ref. 24 shows that a similar trend of marginal variation in lag damping with forward speed for swept tip blade configuration was observed in the experiment.

5. CONCLUDING REMARKS

In this paper, aeroelastic analysis is performed on realistic hingeless blade with tip sweep of 15 deg. and 30 deg. A systematic study was undertaken to analyse the blade tip sweep effect on lead-lag damping in hover and forward flight condition. The important observations of this study can be summarized as follows.

(i) Natural frequencies of structural dynamic model with tip sweep angles of 15 deg., 30 deg., and 45 deg. are validated with the experimental values of composite beams with tip sweep measured in the vacuum chamber rotor test facility[13].

(ii) Predicted natural frequencies are in good agreement with the experimental data for various sweep angles and RPM's.

(iii) For a hingeless straight rotor blade, theoretically (CAFDAR) predicted rotor thrust, power and root loads (flap, lag and torsional) over the entire collective pitch range closely match with the experimental values measured in isolated rotor whirl tower test.

(iv) For a straight blade in hover, the predicted blade lag damping values show a good correlation with the measured values particularly at lower collective pitch angles. At higher collective angles predicted damping values are slightly higher than the measured values.

(v) For a straight blade in forward flight, the blade lag damping value increases with increase in rotor collective pitch angle. It is also observed that the damping shows a slight increase and decrease with increase in advance ratio. This kind of variation in damping qualitatively matches with experimentally observed trend[24].

(vi) Tip sweep influences the blade natural frequencies in all modes. It is also noticed from mode shapes that at higher frequencies there is a coupling between blade flap and lag degrees of freedom with torsional degree of freedom.

(vii) Blade thrust and power marginally decrease with tip sweep angle compared to a straight blade.

(viii) In hover and forward speeds, the blade lead lag damping decreases with increase in sweep angle for all collective angle settings.

(ix) For a swept tip blade in forward flight, blade lag damping value increases with increase in collective angle. It is also noticed that the blade damping shows a marginal increase at lower advance ratios up to 0.1 and then decreases in the range of advance ratios 0.1 to 0.2 and thereafter it shows an increasing trend. This kind of variation of damping trend qualitatively agrees with the experimental observations[24].

6. REFERENCES

[1] Brocklehurst, A., and Barakos, G. N., "A Review of Helicopter Rotor Blade Tip Shapes," Progress in Aerospace Sciences, Vol. 56, pp. 35–74, Jan 2013.

[2] Philippe, J.J., and Vuillet, A., "Aerodynamic Design of Advanced Rotors With New Tip Shapes," Proceedings of the 39th Annual Forum of the American Helicopter Society, pp. 267-277, St.Louis, MO, May 1983.

[3] Yen, J.G., "Effects of blade tip shape on dynamics, cost, weight, aerodynamic performance, and aeroelastic response," Journal of the American Helicopter Soc, Vol.39 (4), pp 37-45, October 1994.

[4] Weller, W. H., "Experimental Investigation of Effects of Blade Tip Geometry on Loads and Performance for an Articulated Rotor System," NASA-TP-1303, 1979.

[5] Stroub, R. H., Rabbott, J. P. and Niebanck, C. F., "Rotor Blade Tip Shape Effects on Performance and Control Loads from Full-Scale Wind Tunnel Testing," Journal of the American Helicopter Society, Vol. 24 (4), pp. 28–35, 1979.

[6] Tarzanin, F.J., Jr., and Vlaminck R.R., "Investigation of the Effect of Blade Sweep on

Presented at 47th European Rotorcraft Forum, United Kingdom, 7-9th September, 2021

Rotor Vibratory loads," NASA CR-166526, October 1983.

[7] Celi, R., and Friedmann, P.P., "Aeroelastic Modeling of Swept Tip Rotor Blades Using Finite Elements," Journal of the American Helicopter Society, Vol.33 (2), April 1988.

[8] Panda, B., "Technical note: Assembly of Moderate-Rotation Finite Elements Used in Helicopter Rotor Dynamics," Journal of the American Helicopter Society, Vol.32 (4), 1987.

[9] Kim, K.C., and Chopra, I., "Aeroelastic Analysis of Swept, Anhedral, and Tapered Tip Rotor Blades," Journal of the American Helicopter Society, Vol. 37 (1), pp. 15-30, 1992.

[10] Friedmann, P.P., Venkatesan C. and Yuan K., "Development of Structural Optimization for the Aeroelastic Tailoring of Composite Rotor Blades with Straight and Swept Tips," presented at the Fourth AIAA/USAF/NASA/OAI Symposium on Multidisciplinary Analysis and Optimization, Cleveland, OH, September 21-23 1992.

[11] Bir, G.S., and Chopra, I., "Aeromechanical stability of rotorcraft with Advance Geometry Blades," 34th AIAA Structural Dynamics and Materials Conference, La Jolla, California, April 1993.

[12] Kumar, M.R., and Venkatesan, C., "Effects of rotor blade-tip geometry on helicopter trim and control response," The Aeronautical Journal, pp.1-23, 2017.

[13] Epps, J.J. and Chandra, R. "The natural frequencies of rotating composite beams with tip sweep," Journal of American Helicopter Soc, Vol. 41 (1), pp 29-36, 1996.

[14] Hopkins, A.S., and Ormiston, R.A., "An Examination of Selected Problems in Rotor Blade Structural Mechanics and Dynamics," Proceedings American Helicopter Society 59th Annual Forum, 2003.

[15] D.H. Hodges and E.H. Dowell, "Nonlinear Equations of Motion for the Elastic Bending and Torsion of Twisted Nonuniform Rotor Blades," NASA TN D-7818 (1974).

[16] Amoozgar, M.R., Shaw, A.D., and Friswell, M.I., "The effect of curved tips on the dynamics of composite rotor blades," Journal of Aerospace Science and Technology, 106(6), Nov. 2020.

[17] Perry, F. J., "Aerodynamics of the Helicopter World Speed Record," Proceedings of 43rd Annual Forum of the American Helicopter Society, AHS International, Fairfax, VA, pp. 3–15, 1987.

[18] Rauch, P., Gervais, M., Cranga, P., Baud, A., Hirsch, J.,Walter, A., and Beaumier, P., "Blue Edge: The Design, Development and Testing of a New Blade Concept," Proceedings of the 67th Annual Forum of the American Helicopter Society, AHS International, Fairfax, VA, pp. 542–555, 2011.

[19] Van der Wall, B., Kessler, C., Pengel, K., Gervais, M., Hirsch, J., Delrieux, Y., Beaumier, P., and Crozier, P., "From ERATO Basic Research to the Blue Edge Rotor Blade," Proceedings of 72nd Annual Forum of the American Helicopter Society, AHS International, Fairfax, VA, pp. 3103–3121, 2016.

[20] Truong, K.V., "Dynamics Studies of the ERATO Blade, Based on Finite Element Analysis," Proceedings of the 31st European Rotorcraft Forum, Associazione Italiana di Aeronautica e Astronautica, Rome, pp. 1122–1133, 2005.

[21] Kumar, M. R., and Rao, L., "Aeroelastic Analysis of Double-Swept Rotor Blade in Hovering Conditions," Proceedings of 17th International Forum on Aeroelasticity and Structural Dynamics, Curran Associates Inc., Como, Italy, pp. 1318–1331, 2017.

[22] Filippi, M., Zappino, E., and Carrera, E., "Multidimensional Models for Double-Swept Helicopter Blades," AIAA Journal, Vol. 57 (6), pp. 2609–2616, 2019.

[23] Zhang, J., Xia, P., and Chopra, I., "Aeromechanical Stability of Bearingless Rotor Helicopter with Double-Swept blades," Journal of Aircraft, Vol. 58 (2), pp. 242–252, 2021.

[24] Maier, T. H., Sharpe, D. L., and Abrego, A. I., "Aeroelastic Stability for Straight and Swept-Tip Rotor Blades in Hover and Forward Flight," Proceedings of 55th Annual Forum of American Helicopter Society, AHS International, Fairfax, VA, pp. 1031–1047, 1999.

[25] Kumar, M.R. and Venkatesan, C. "Rotorcraft aeroelastic analysis using dynamic wake/dynamic stall models and its validation," Journal of Aeroelasticity and Structural Dynamics, Vol. 3 (1), 2013.

[26] Peters, D. A., and He, C. J., "Correlation of Measured Induced Velocities with a Finite-State Wake Model", Journal of the American Helicopter Society," Vol 36 (3), pp.59-70, 1991.

[27] Laxman, V., and Venkatesan, C., "Influence of dynamic stall and dynamic wake effects on helicopter trim and rotor loads," Journal of the American Helicopter Society, Vol 54 (3), July 2009.

Presented at 47th European Rotorcraft Forum, United Kingdom, 7-9th September, 2021

[28] GSL – GNU Scientific Library, Available at URL: http://www.gnu.org/software/gsl/.

[29] Bielawa R L. “Rotary wing structural dynamics and aeroelasticity”, America: AIAA, Inc, Washington, DC, 475-479, 1992.

[30] Smith C B, and Wereley N M. “Damping identification in helicopter rotor system”, Proceedings of the American Helicopter Society, 54th Annual Forum, Washington DC, 1998.

[31] Bir, G. S., Wright, A. D., and Butterfield, C. P., “Stability Analysis of Variable Speed Wind Turbine,” ASME Wind Energy Symposium, Reno, Nevada, January 1997.

[32] Hu, G. C., Zhang, X. G., and Xiang, J. W., “Dynamic Stability Analysis for Helicopter Rotor/ Fuselage Coupled Nonlinear Systems,” Chinese Journal of Aeronautics, Vol 16 (1), 2003.

[33] Rainer Vorwerg., “Development of an Advanced Experimental Rotary Test Rig and First Test Results With a 60 kN-Main Rotor,” 14th European Rotor Forum, Milano, Italy, September 1988.

[34] Rutvik, C., “Sectional Properties of Beam-Type Composite Structures with Arbitrary Cross-Section,” M.Tech Thesis, Department of Aerospace Engineering, IIT Kanpur, 2015.

Presented at 47th European Rotorcraft Forum, United Kingdom, 7-9th September, 2021

Table 2: Details of Experimental Swept-tip beams (Ref. [13])

S.NO	Material	Sweep (deg)	Lay-up	Thickness (mm)	Width (mm)
1	Aluminum (E = 70 GPa , μ = 0.3)	0	-	1.60	25.4
		15	-	1.60	25.4
		30	-	1.60	25.4
		45	-	1.60	25.4
2	Graphite-epoxy (E_l = 142 GPa, E_t = 9.70 GPa , G_{lt} = 5.86 GPa , μ_{lt} = 0.42)	0	$[0]_{24}$	2.97	25.4
		15		3.05	25.4
		30		3.07	25.4
		45		3.07	25.4
		0	$[15]_{24}$	3.07	25.4
		15		3.12	25.4
		30		3.12	25.4
		45		3.23	25.4
		0	$[30]_{24}$	3.07	25.4
		15		3.10	25.4
		30		3.10	25.4
		45		3.12	25.4

Table 3: Cross-sectional properties of experimental swept-tip beams

Material		Sweep (deg)	Thickness (mm)	Mass (Kg/m)	Flap Inertia (Kg-m)	Lag Inertia (Kg-m)	Axial Stiffness (N)	Flap Stiffness (Nm^2)	Lag Stiffness (Nm^2)	Torsional Stiffness (Nm^2)
Aluminum		0	1.60	0.110	2.34E-08	5.90E-06	2.84E+06	0.67	153.04	1.09
		15	1.60	0.110	2.34E-08	5.90E-06	2.84E+06	0.67	153.04	2.09
		30	1.60	0.110	2.34E-08	5.90E-06	2.84E+06	0.67	153.04	3.09
		45	1.60	0.110	2.34E-08	5.90E-06	2.84E+06	0.67	153.04	4.09
Graphite-epoxy	$[0]_{24}$	0	2.97	0.121	8.90E-08	6.51E-06	1.07E+07	7.87	575.90	1.21
		15	3.05	0.123	9.64E-08	6.68E-06	1.10E+07	8.53	591.44	1.30
		30	3.07	0.125	9.83E-08	6.73E-06	1.11E+07	8.69	595.32	1.33
		45	3.07	0.125	9.83E-08	6.73E-06	1.11E+07	8.69	595.32	1.33
	$[15]_{24}$	0	3.07	0.125	9.83E-08	6.73E-06	7.78E+06	6.71	246.70	2.73
		15	3.12	0.127	1.03E-07	6.84E-06	7.91E+06	7.03	250.70	2.86
		30	3.12	0.127	1.03E-07	6.84E-06	7.91E+06	7.03	250.70	2.86
		45	3.23	0.132	1.14E-07	7.08E-06	8.18E+06	7.78	259.54	3.16
	$[30]_{24}$	0	3.07	0.125	9.83E-08	6.73E-06	3.40E+06	2.97	100.76	3.58
		15	3.10	0.126	1.01E-07	6.79E-06	3.45E+06	3.05	101.74	3.68
		30	3.10	0.126	1.01E-07	6.79E-06	3.45E+06	3.05	101.74	3.68
		45	3.12	0.127	1.03E-07	6.84E-06	3.47E+06	3.11	102.39	3.75

Table 4: Natural frequencies (/rev) of a realistic blade with tip sweep

Mode No	Straight blade	Tip-Sweep 15deg	Tip-Sweep 30deg	Predominant Mode
1	0.683	0.674	0.645	1st Lag
2	1.079	1.075	1.060	1st Flap
3	2.656	2.638	2.581	2nd Flap
4	4.698	4.667	4.569	2nd Lag
5	4.889	4.824	4.661	3rd Flap
6	5.571	5.648	5.798	1st Torsion
7	7.605	7.613	7.656	4th Flap
8	40.089	40.109	40.146	1st Axial

Presented at 47th European Rotorcraft Forum, United Kingdom, 7-9th September, 2021

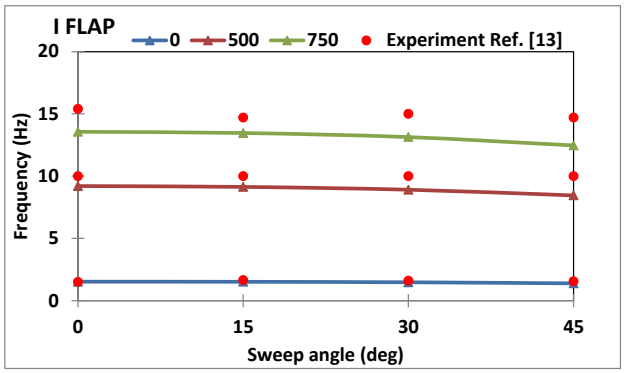

Figure 5: The influence of tip sweep and rotational speed on the natural frequencies of aluminium beams: first flap bending mode.

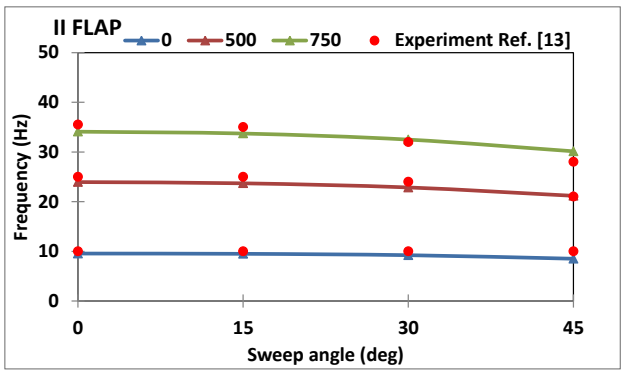

Figure 6: The influence of tip sweep and rotational speed on the natural frequencies of aluminium beams: second flap bending mode.

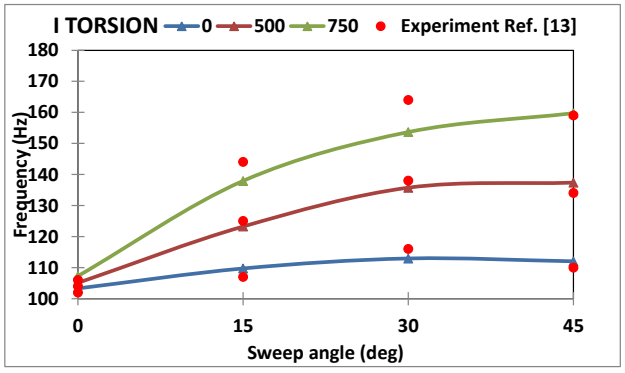

Figure 7: The influence of tip sweep and rotational speed on the natural frequencies of aluminium beams: first torsion mode.

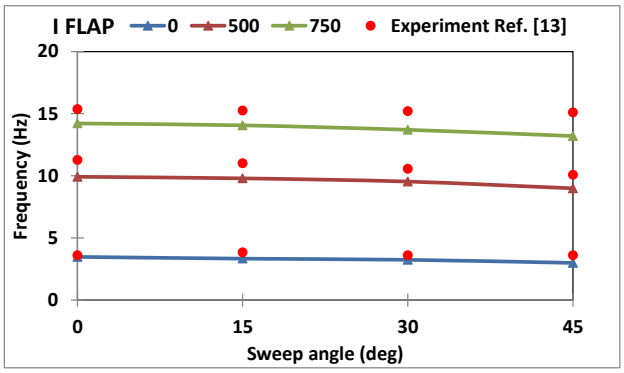

Figure 8: The influence of tip sweep and rotational speed on the natural frequencies of graphite-epoxy beams, $[0]_{24}$: first flap bending mode.

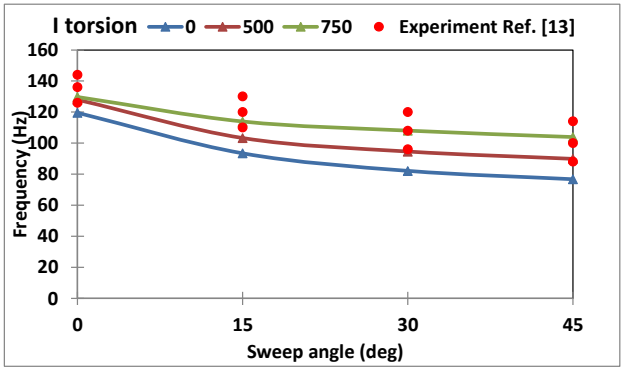

Figure 9: The influence of tip sweep and rotational speed on the natural frequencies of graphite-epoxy beams, $[0]_{24}$: first torsion mode.

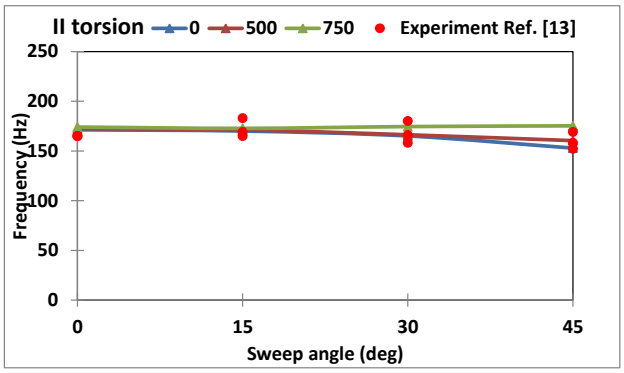

Figure 10: The influence of tip sweep and rotational speed on the natural frequencies of graphite-epoxy beams, $[0]_{24}$: second torsion mode.

Presented at 47th European Rotorcraft Forum, United Kingdom, 7-9th September, 2021

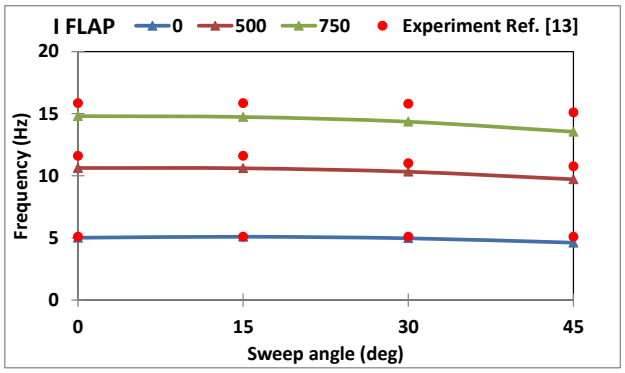

Figure 11: The influence of tip sweep and rotational speed on the natural frequencies of graphite-epoxy beams, $[15]_{24}$: first flap mode.

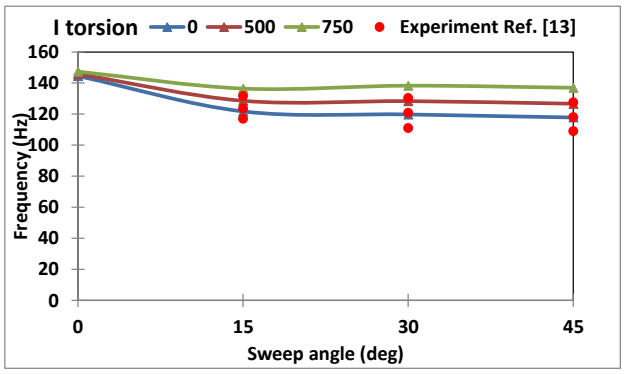

Figure 12: The influence of tip sweep and rotational speed on the natural frequencies of graphite-epoxy beams, $[15]_{24}$: first torsion mode.

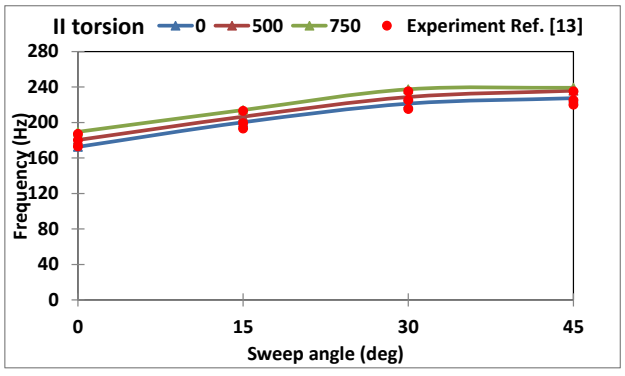

Figure 13: The influence of tip sweep and rotational speed on the natural frequencies of graphite-epoxy beams, $[15]_{24}$: second torsion mode.

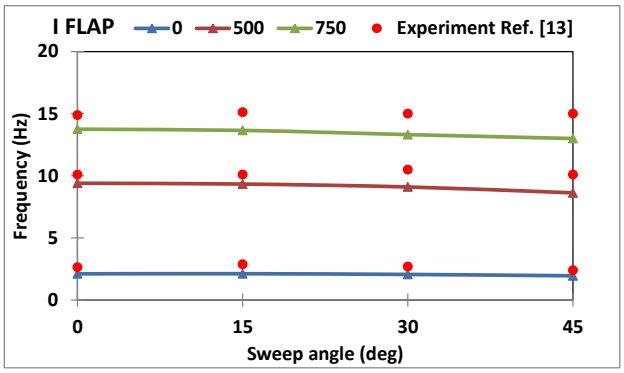

Figure 14: The influence of tip sweep and rotational speed on the natural frequencies of graphite-epoxy beams, $[30]_{24}$: first flap mode.

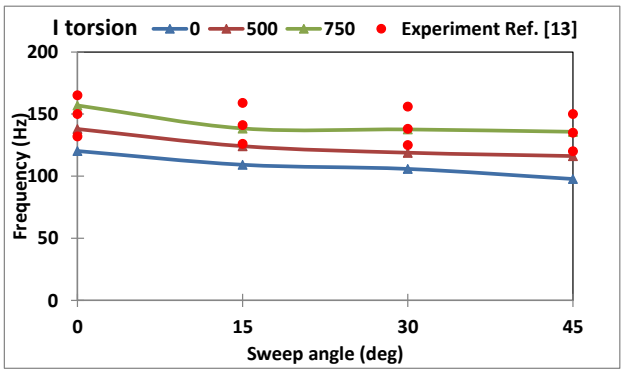

Figure 15: The influence of tip sweep and rotational speed on the natural frequencies of graphite-epoxy beams, $[30]_{24}$: first torsion mode.

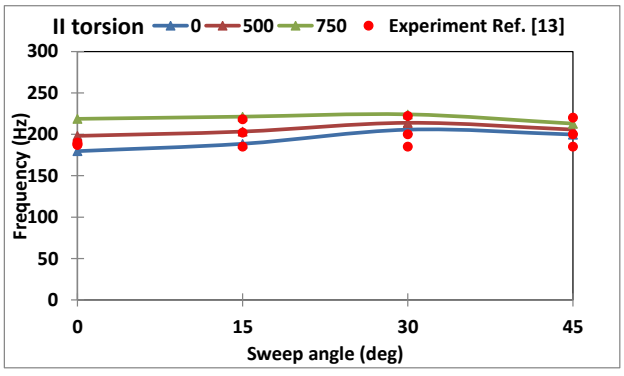

Figure 16: The influence of tip sweep and rotational speed on the natural frequencies of graphite-epoxy beams, $[30]_{24}$: second torsion mode.

Presented at 47th European Rotorcraft Forum, United Kingdom, 7-9th September, 2021

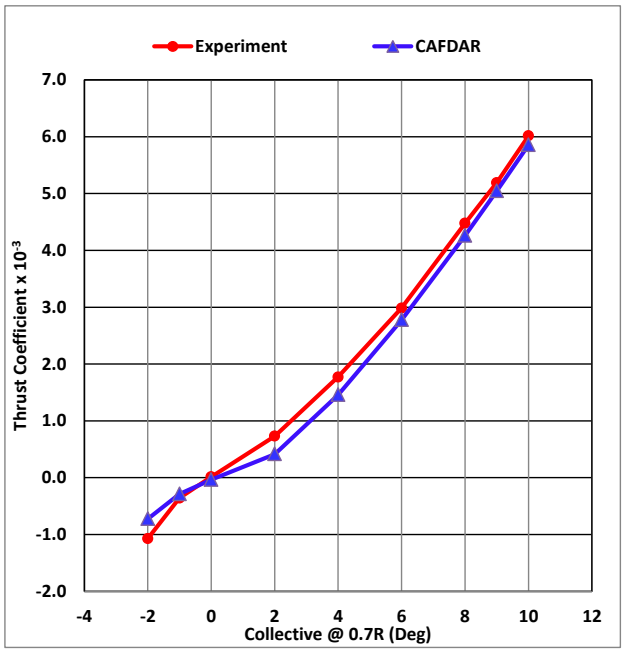

Figure 17: Comparison of rotor thrust for a straight blade (experimental data with CAFDAR calculations for various collective angles).

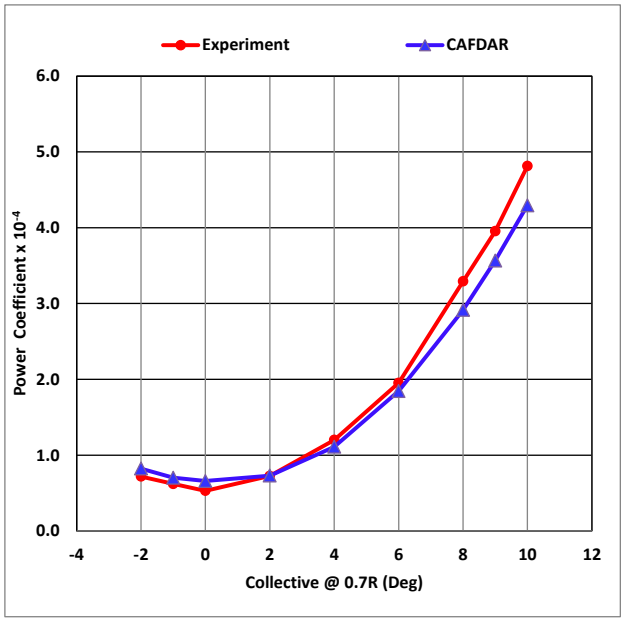

Figure 18: Comparison of rotor power for a straight blade (experimental data with CAFDAR calculations for various collective angles).

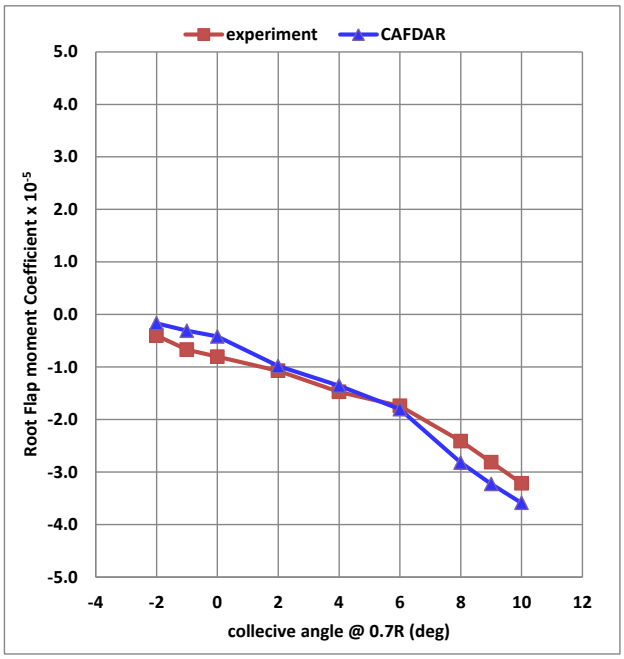

Figure 19: Comparison of blade root flap moment at station #465 for a straight blade (Experimental data with CAFDAR calculations for various collective angles)

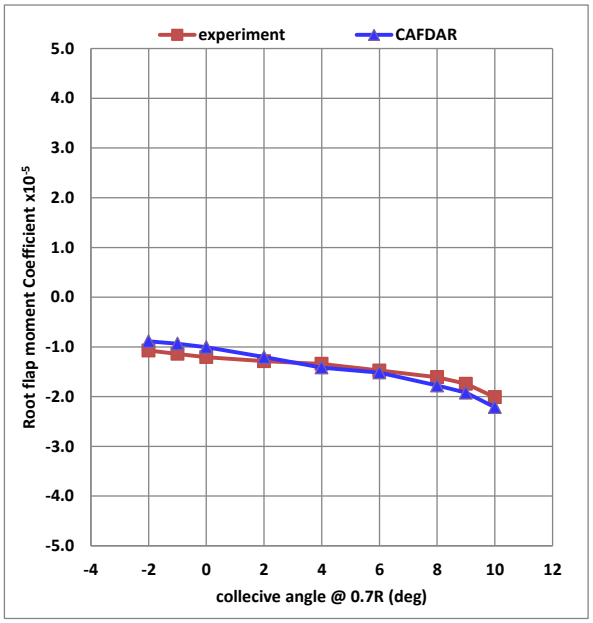

Figure 20: Comparison of blade root flap moment at station #850 for a straight blade (Experimental data with CAFDAR calculations for various collective angles).

Presented at 47th European Rotorcraft Forum, United Kingdom, 7-9th September, 2021

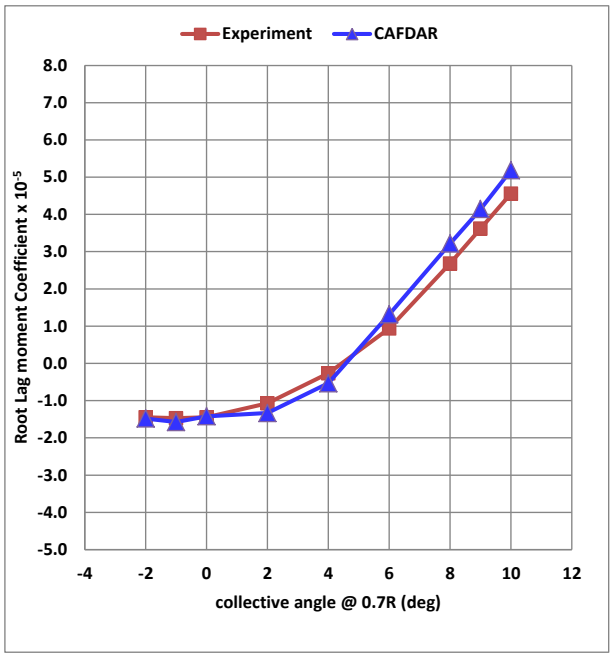

Figure 21: Comparison of blade root lag moment at station #465 for a straight blade (Experimental data with CAFDAR calculations for various collective angles).

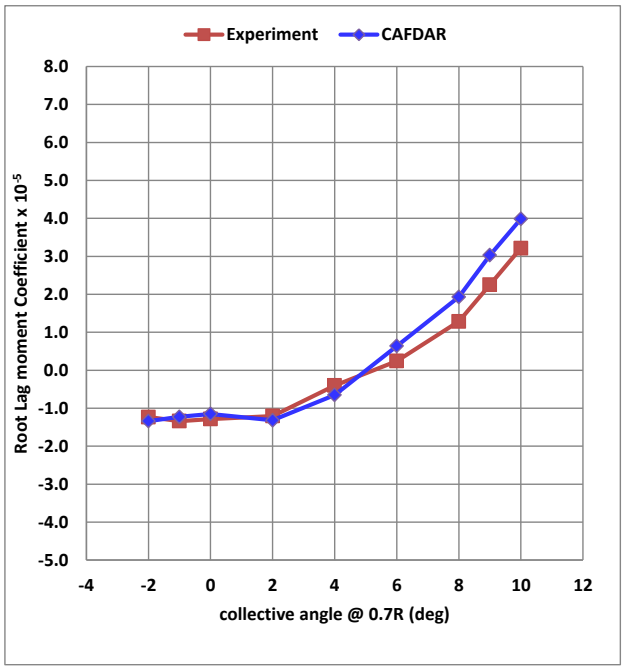

Figure 22: Comparison of blade root lag moment at station #850 for a straight blade (Experimental data with CAFDAR calculations for various collective angles).

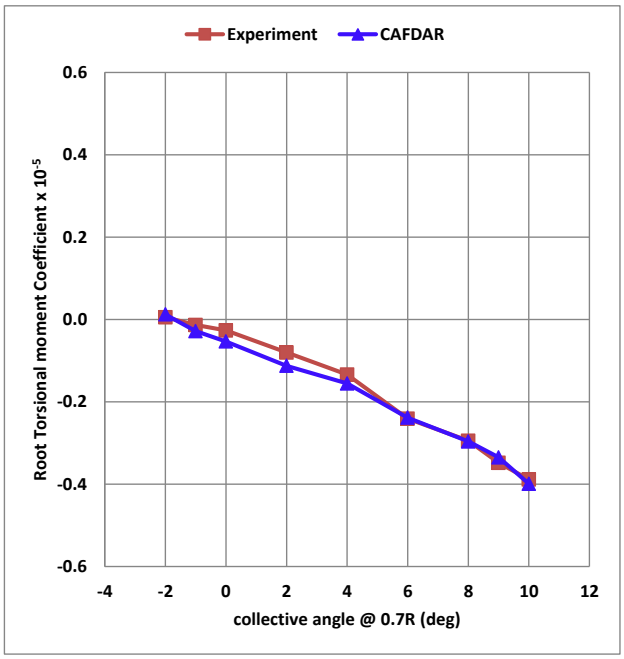

Figure 23: Comparison of blade root torsional moment for a straight blade (Experimental data with CAFDAR calculations for various collective angles).

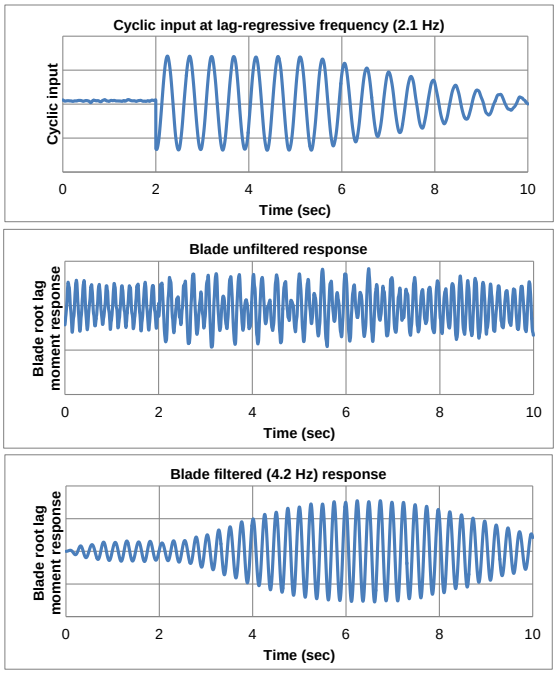

Figure 24: Cyclic input and blade root in-plane moment response on whirl tower test.

Presented at 47th European Rotorcraft Forum, United Kingdom, 7-9th September, 2021

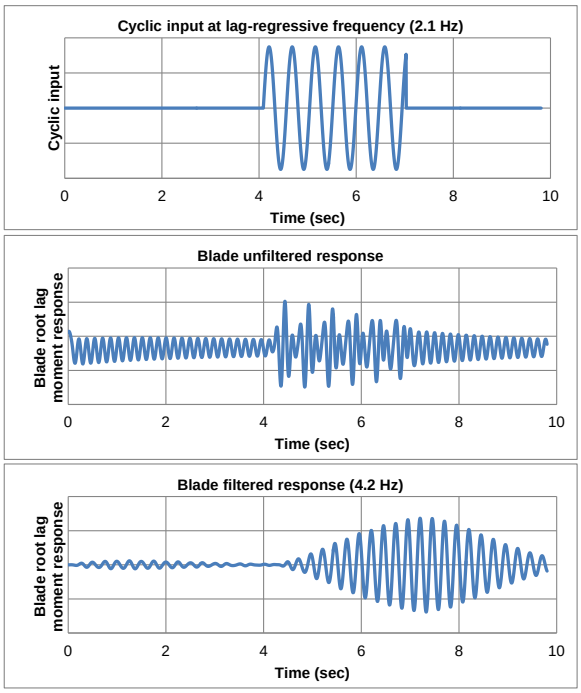

Figure 25: Cyclic input and blade root in-plane moment response in CAFDAR.

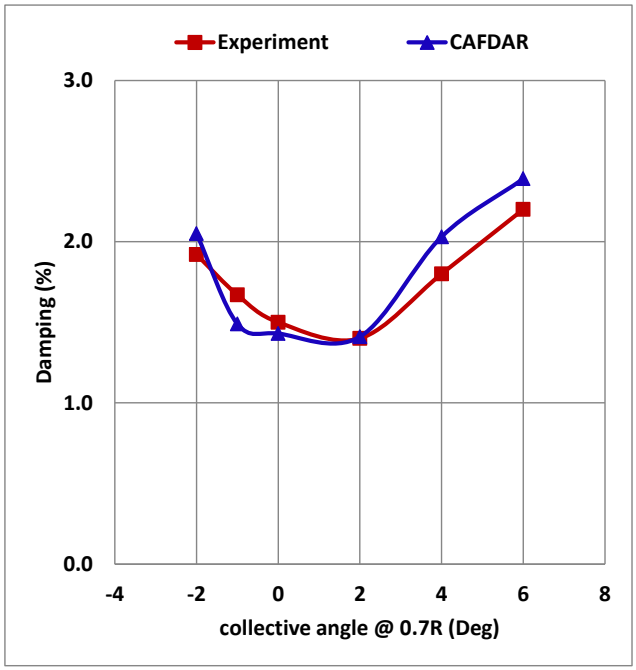

Figure 26: Comparison of lag damping for a straight blade (Experimental data with CAFDAR calculations for various collective angles.

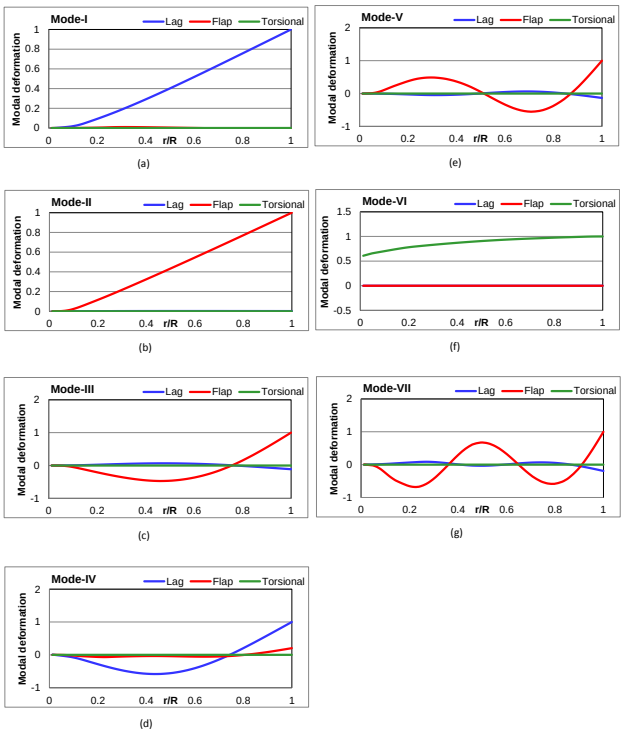

Figure 27: Straight blade mode shapes.

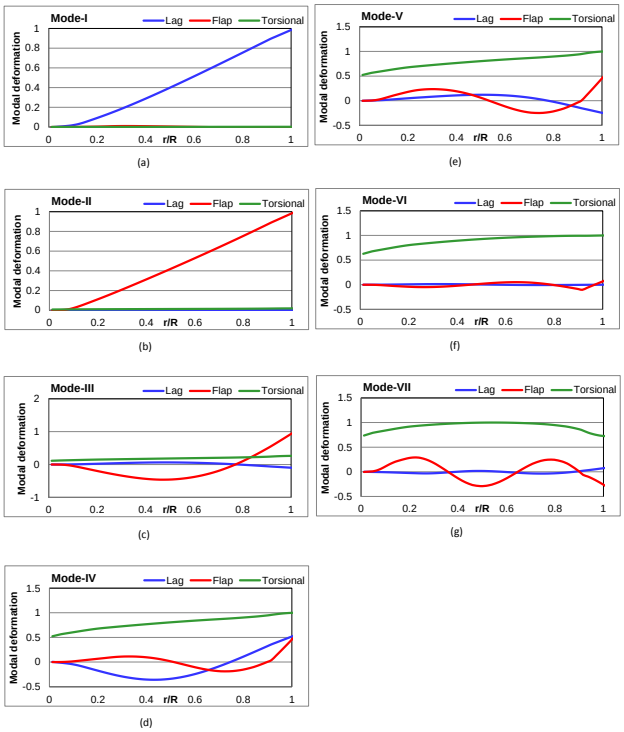

Figure 28: Blade mode shapes for a swept tip of 30 deg.

Presented at 47th European Rotorcraft Forum, United Kingdom, 7-9th September, 2021

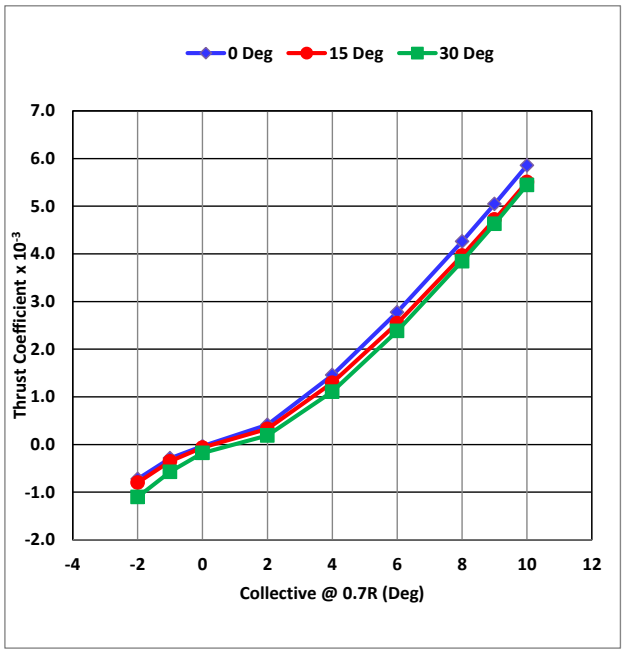

Figure 29: Comparison of rotor thrust variation with blade tip sweep angles (CAFDAR calculations for various collective angles).

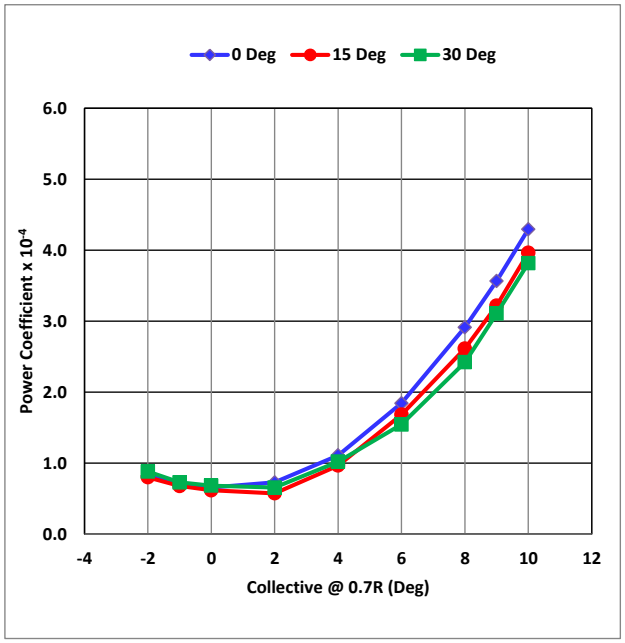

Figure 30 Comparison of rotor power variation with blade tip sweep angles (CAFDAR calculations for various collective angles).

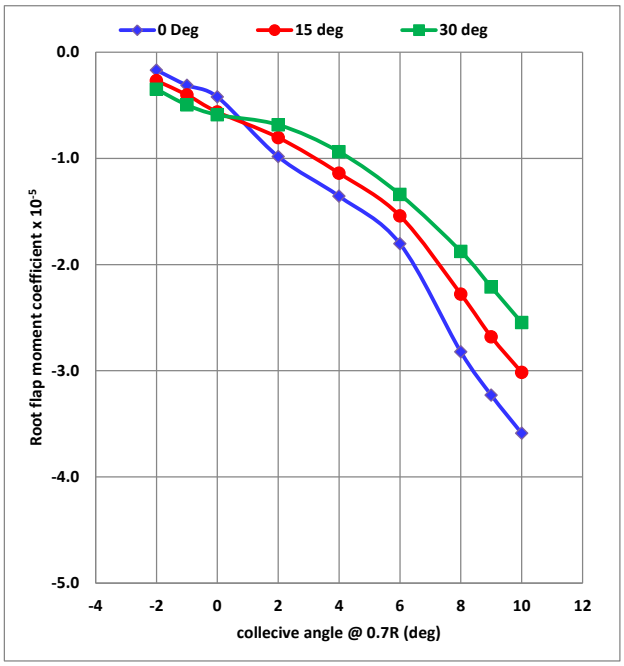

Figure 31: Comparison of blade root flap moment at station #465 with blade tip sweep angles (CAFDAR calculations for various collective angles).

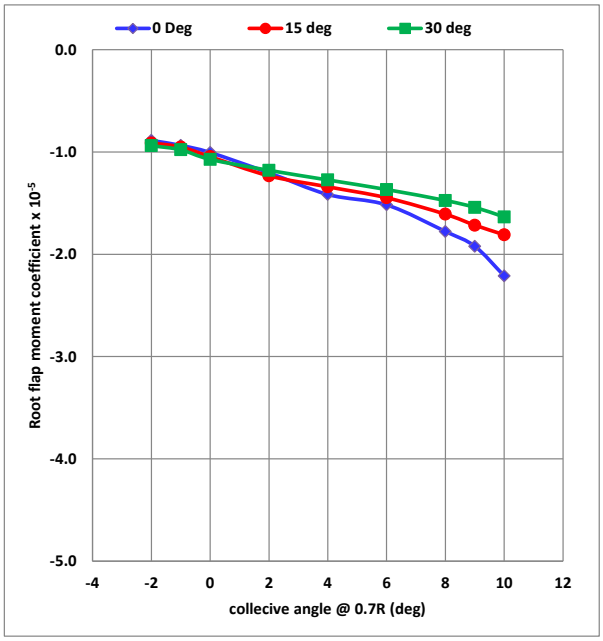

Figure 32: Comparison of blade root flap moment at station #850 with blade tip sweep angles (CAFDAR calculations for various collective angles).

Presented at 47th European Rotorcraft Forum, United Kingdom, 7-9th September, 2021

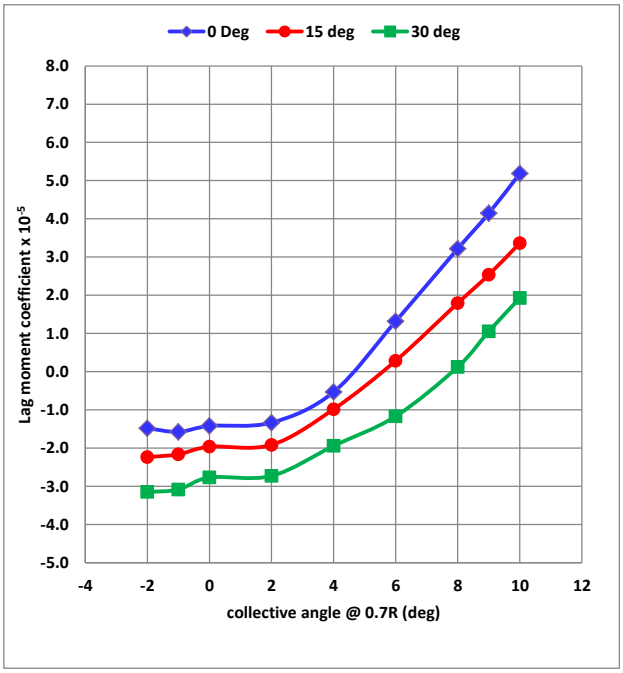

Figure 33: Comparison of blade root lag moment at station #465 with blade tip sweep angles (CAFDAR calculations for various collective angles).

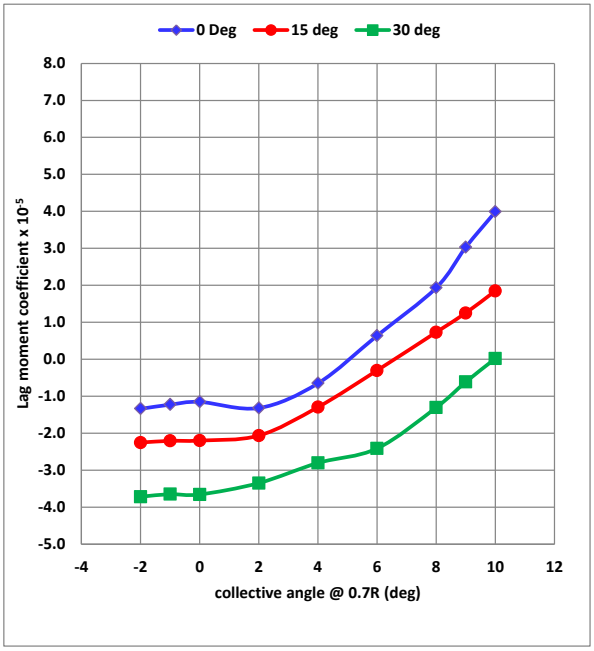

Figure 34: Comparison of blade root lag moment at station #850 with blade tip sweep angles (CAFDAR calculations for various collective angles).

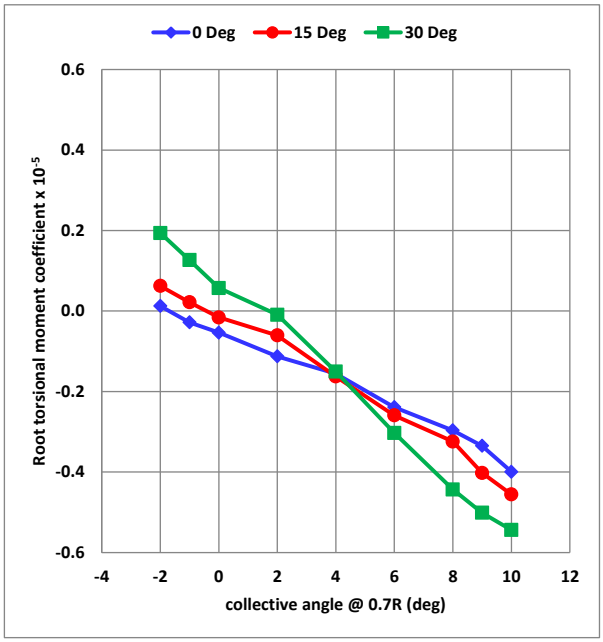

Figure 35: Comparison of blade root torsional moment with blade tip sweep angles (CAFDAR calculations for various collective angles).

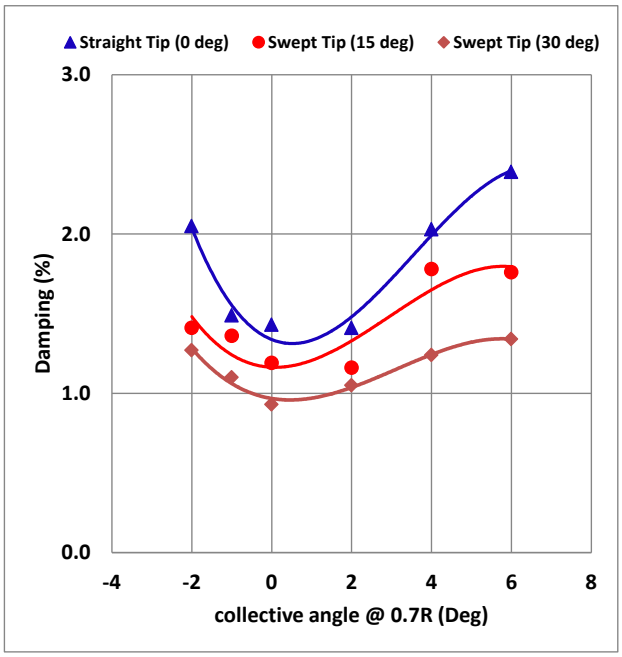

Figure 36: Comparison of lag damping in hover for straight and swept tip blades (CAFDAR calculations for various collective angles).

Presented at 47th European Rotorcraft Forum, United Kingdom, 7-9th September, 2021

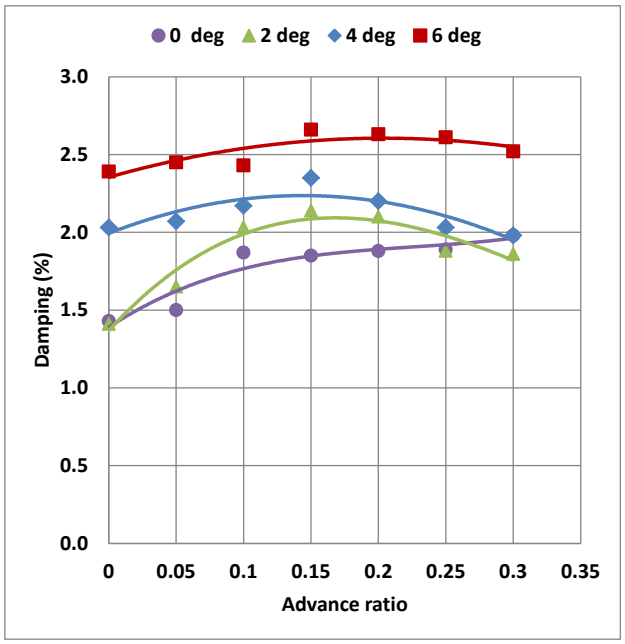

Figure 37: Variation of blade lag damping with forward speed for straight blade (CAFDAR calculations for various collective angles).

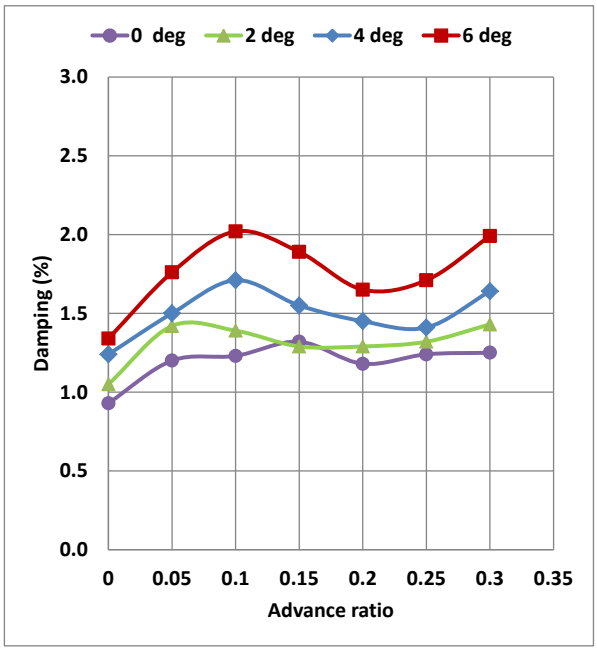

Figure 39: Variation of blade lag damping with forward speed for 30 deg. swept tip blade (CAFDAR calculations for various collective angles).

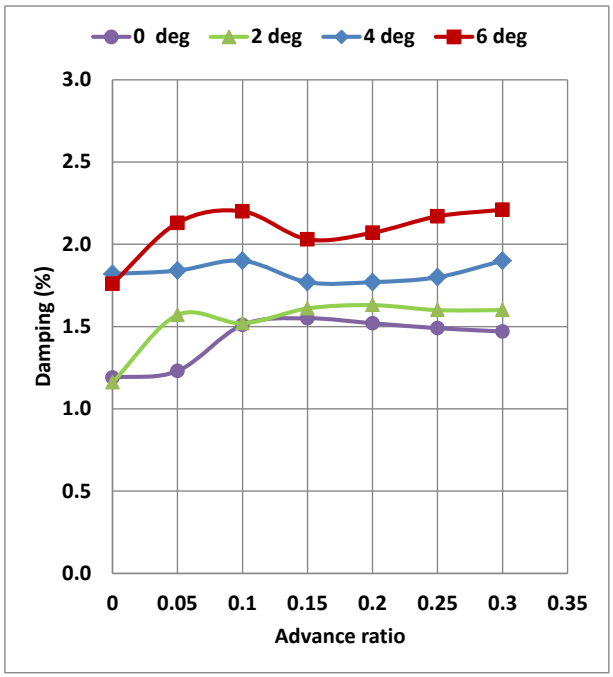

Figure 38: Variation of blade lag damping with forward speed for 15 deg. swept tip blade (CAFDAR calculations for various collective angles).

Presented at 47th European Rotorcraft Forum, United Kingdom, 7-9th September, 2021